Electronic distribution in the Ba_2FeMoO_6 double perovskite; the A-site size effect

2002 J. Phys.: Condens. Matter 14 12629

(http://iopscience.iop.org/0953-8984/14/47/333)

INSTITUTE OF PHYSICS PUBLISHING JOURNAL OF PHYSICS: CONDENSED MATTER

J. Phys.: Condens. Matter **14** (2002) 12629–12640 PII: S0953-8984(02)33192-8

Electronic distribution in the Ba_2FeMoO_6 double perovskite; the A-site size effect

N Nguyen[1,4], F Sriti[1], C Martin[1], F Bourée[2], J M Grenèche[3], A Ducouret[1], F Studer[1] and B Raveau[1]

[1] Laboratoire CRISMAT, UMR 6508 Associée au CNRS, ISMRA et Université de Caen, 6 Boulevard du Maréchal Juin, 14050 Caen Cedex, France
[2] LLB-Saclay, 91151 Gif sur Yvette Cedex, France
[3] Laboratoire de Physique de l'Etat Condensé, UMR CNRS 6087, Université du Maine, 72085 Le Mans Cedex 9, France

E-mail: ninh.nguyen@ismra.fr

Received 30 January 2002, in final form 1 October 2002
Published 15 November 2002
Online at stacks.iop.org/JPhysCM/14/12629

Abstract

The double perovskite Ba_2FeMoO_6 has been studied by neutron powder diffraction, Mössbauer spectrometry and x-ray absorption spectroscopy, and is compared with Sr_2FeMoO_6. It is shown that the size of the A-site cation has a large effect upon the nature of the low-temperature state, favouring the majority Fe^{2+}/Mo^{6+} pair in the case of barium and the Fe^{3+}/Mo^{5+} pair in the case of strontium. In both cases, an electronic transfer appears as T decreases, interpreted as the existence of a minority $t_{2g}\downarrow$ narrow band, where the electron is itinerant.

1. Introduction

The double perovskites A_2FeMoO_6 (A = Sr, Ba), synthesized for the first time almost 40 years ago [1, 2], were recently found to be half-metallic ferromagnets showing large magnetoresistance, especially tunnel magnetoresistance (TMR), at room temperature [3, 4], suggesting promising applications. Thus, knowledge of the Fe–O–Mo bond is of great importance for understanding the properties of these oxides.

Numerous investigations have been carried out for Sr_2FeMoO_6, which exhibits the highest T_C of 422 K, using either Mössbauer spectrometry [5–7] or neutron diffraction [8, 9]. Mössbauer spectra are usually described by a discrete number of components attributed to different types of iron neighbour. The results of the Mössbauer studies vary from one author to the other: Nakagawa [5] observed a majority of Fe^{3+}, whereas Lindén *et al* [6] and Grenèche *et al* [7] found a valence fluctuation corresponding to $Fe^{2.5+}$ and $Fe^{2.8+}$ respectively. But more importantly, a fundamental discrepancy is found between the Mössbauer studies and the

[4] Author to whom any correspondence should be addressed.

neutron diffraction studies [8, 9], the latter showing a magnetic moment close to 4 μ_B for Fe sites, supporting an Fe^{2+} electronic configuration instead of $Fe^{2.5+}$ or $Fe^{2.8+}$. Such an apparent disagreement between the Mössbauer and neutron diffraction results is generally explained by the itinerant t_{2g} electrons of Mo, which would be spin-down and can hop through the oxygen orbital to the spin-up t_{2g} Fe orbital, so that the magnetic moment of Fe^{3+}(5 μ_B) would be reduced. The great difficulty in understanding these data arises from the method of synthesis used by different authors which may modify the cationic ordering and the oxygen and cationic stoichiometries. It has indeed been shown that there often exists a partial disordering of the Mo and Fe cations which means that the magnetic moment observed at saturation is lower than the theoretical value [3, 10–12].

In contrast to the Sr compound, Ba_2FeMoO_6 has not been intensively investigated, due to its lower T_C of 334 K [2]. A previous neutron diffraction study of this phase showed a significant deviation from the stoichiometry, leading to the formula $Ba_2Fe_{0.92}Mo_{0.93}O_{5.69}$ [9]. A Mössbauer study [7] showed a $Fe^{2.5+}$ state deduced from the isomer shift (IS) at 4.2 K, but the corresponding hyperfine field value was not discussed. More recently, a fitting model based on a fluctuating magnetic field was proposed to describe low- and high-temperature Mössbauer absorption spectra [13], but unfortunately the simulated spectra of these authors do not fit well with the observed spectra, as far as the broadening of the lines is concerned. In the present work this phase was revisited: a neutron powder diffraction (NPD) study at 10 and 450 K, a Mössbauer study at 80 K and x-ray absorption spectroscopy were performed on the same sample. All methods convergently demonstrate that in Ba_2FeMoO_6 the major interactions are of the Fe^{2+}–O–Mo^{6+} type. Compared with Sr_2FeMoO_6, for which the major interactions correspond to Fe^{3+}–O–Mo^{5+}, it is shown that, as previously reported, the size of the A-site cation affects the crystalline structure [9] but also the nature of the major species, i.e. the electronic distribution, even if it does not hinder the itinerant carriers, lowering only T_C.

2. Experimental section

The Ba_2FeMoO_6 and Sr_2FeMoO_6 samples were prepared by solid state reaction, starting from BaO_2 or SrO_2, Fe_2O_3, MoO_3 and Mo in amounts calculated in order to respect the cationic ratio and the 'O_6' content. The powders were pressed in the form of bars and heated in evacuated silica ampoules at 1200 °C for 12 h.

The x-ray powder diffraction (XRPD) patterns were registered at room temperature with a Philips diffractometer using Cu Kα radiation. Neutron experiments were carried out at LLB-Saclay (France) on the 3T2 diffractometer ($\lambda = 1.2251$ Å and in the angular range 6°–125° in 2θ) at 450 and 10 K for the Ba_2FeMoO_6 compound. Crystallographic and magnetic structures were analysed by the Rietveld method using the Fullprof program.

The magnetization measurements ($M(T)$) were performed in the range 5–400 K using a dc SQUID Quantum Design magnetometer (zero-field cooled (ZFC) method) with an applied field of 1.45 T.

Mössbauer absorption powder spectra were recorded using a constant-acceleration conventional spectrometer with a ^{57}Co/Rh source. For the prepared samples without the thickness effect, we have least-squares fitted the spectra with a Lorentzian line shape using the computer program MOSFIT [14]. The IS values are quoted relative to that of α-Fe at 300 K.

The x-ray absorption spectra at the Mo K-edge (20 keV) were recorded at room temperature in a classical transmission mode at the EXAFS (extended x-ray absorption fine structure) I station (channel cut monochromator) using the synchrotron radiation of the DCI storage ring of LURE (Orsay) working at 1.85 GeV with a 250 mA current. The energy resolution at the Mo K-edge is estimated as 7 eV whereas the reproducibility of the monochromator is

as good as 0.3 eV. The normalization procedure used throughout this work was a standard one: after subtraction of the same diffusion background on the XANES (x-ray absorption near-edge structure) and EXAFS spectra, recorded under the same experimental conditions, a point located at an energy of 800 eV from the edge, where no more EXAFS oscillations were observable, was set to unity. Then the intensity of a point with an energy between 50 and 100 eV from the edge was recorded on the EXAFS spectrum and reported on the XANES to set the normalization height.

3. Results and discussion

X-ray diffraction

The room-temperature x-ray diffraction pattern of the sample with nominal composition Ba_2FeMoO_6 was refined in the $Fm3m$ space group with $a = 8.0596(1)$ Å, in agreement with the previous electron diffraction study of this phase [4]. Two impurities were observed, $BaMoO_4$ and $BaCO_3$ with weight fractions of 8 and 3.5% respectively. They were introduced in the calculations with the space groups $I4_1/a$ [15] and $Pmcn$ [16] respectively, as shown figure 1(a). The main result of this study concerns the refinement of the occupancy of the Fe and Mo sites which converged for a Fe/Mo ratio very close to 1 (1.03(1)), in agreement with the EDS (energy dispersive spectroscopy) analysis (Fe/Mo = 1). Attempts to exchange Fe and Mo on both sites did not improve the fit.

Neutron diffraction

In order to be in the paramagnetic state, an NPD pattern was recorded at 450 K (figure 1(b)). In fact, as shown by the magnetization measurements (figure 2) and as previously reported [4], the compound exhibits a ferromagnetic component at low temperature, leading to a magnetic moment of 3.2 μ_B per formula unit at 4 K. The Curie temperature, taken at the inflection point on the $M(T)$ (inset of figure 2) is $\approx$330 K. The corresponding crystallographic parameters (table 1) are in agreement with those obtained from XRPD data, as well the observations concerning the impurities. The important result deals with the oxygen content that is found to be 'O_6' (the oxygen occupancy was refined at 5.98(2)). The refinement of Fe and Mo sites leads to occupancy factors of 1.00(1) for Fe and 0.96(2) for Mo, i.e. close to those obtained from XRPD. The higher accuracy of the distribution of metallic elements obtained from XRPD data shows that occupancy factors of Fe and Mo sites can be given as equal to 1. Thus, this preliminary study is important: it shows that the studied compound is practically stoichiometric, i.e. with the formulation Ba_2FeMoO_6, without any detectable disordering between the Mo and Fe sites, in the limit of accuracy. This composition is thus different from that previously studied by Ritter *et al* [9], which showed significant Fe, Mo and oxygen deficiencies, leading to the formula $Ba_2Fe_{0.92}Mo_{0.93}O_{5.69}$. Such a difference is easily explained by the different methods of synthesis. In our case, the most puzzling point is that no Fe-based impurity was found on the XRPD pattern or by a close inspection of more than 50 crystallites by electron microscopy. Nevertheless, the values obtained for the occupancy factors (from XRPD and NPD data) are a little bit higher for Fe than Mo but are in the limit of the accuracy. Moreover, the existence of a non-crystallized impurity cannot be excluded. Note that similar observations, showing the difficulty of obtaining pure double perovskites and consequently explaining the behaviour of such compounds, are also made by many authors; for instance Ritter *et al* [9] observed Sr_2MoO_6 and $SrMoO_4$ as impurities in their Sr_2FeMoO_6. Nevertheless, due to the reproducibility in the preparation of the samples and also in the characterization results, performing different

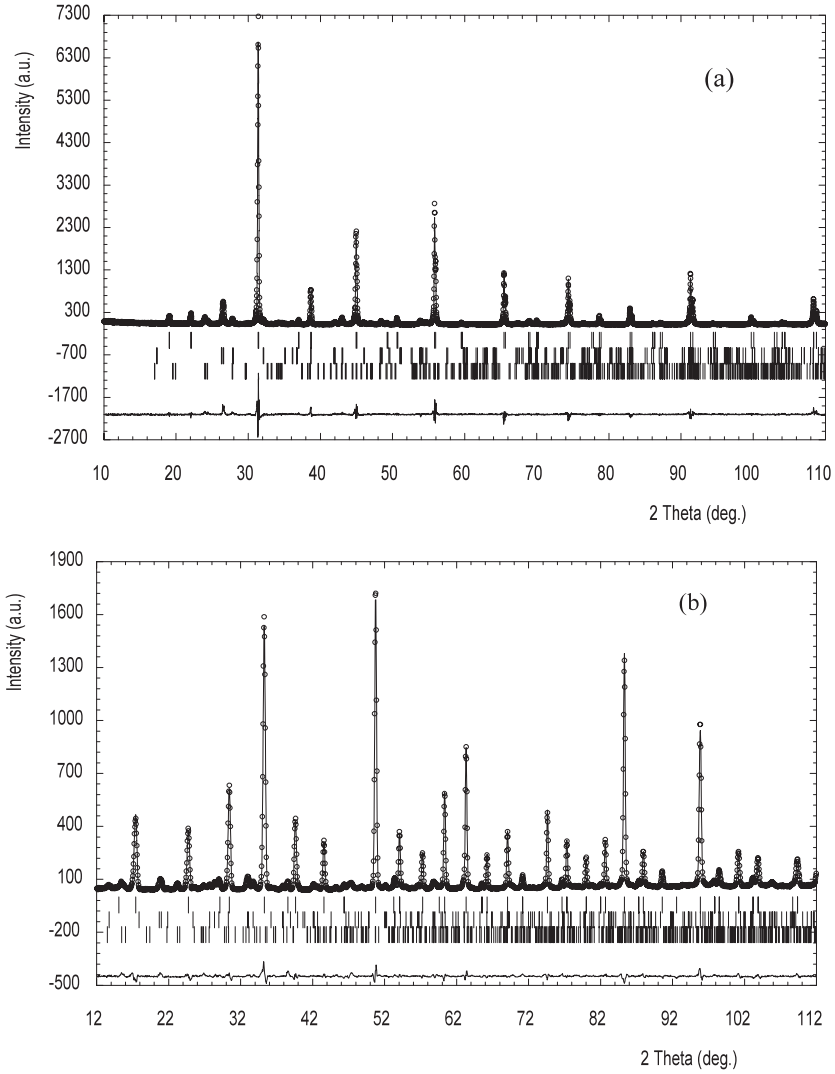

Figure 1. Experimental (circles) and calculated (continuous curve) room-temperature x-ray (a) and 450 K neutron (b) powder diffraction patterns. The Bragg peaks are, from high to low, for Ba_2FeMoO_6 ($Fm3m$), $BaMoO_4$ ($I4_1/a$) and $BaCO_3$ ($Pmcn$). The lower plot is the difference.

types of experiments (x-ray, neutron and electron diffraction, x-ray absorption and Mössbauer spectroscopy) on a *unique* sample allows conclusions to be made.

The low-temperature data (10 K) are rather difficult to refine due to the overlap of the Bragg peaks of the main phase and of the impurities and to the merging of the magnetic and nuclear peaks, as shown figure 3. For instance, the scale factors at low temperature have been fixed at the values obtained at high temperature, which were consistent with those calculated from the room-temperature XRPD data. These refinements show that the structure remains as $Fm3m$ (table 1), the cell parameter decreasing to 8.0506(2) Å. The magnetic structure is in agreement with that previously observed for $Ba_2Fe_{0.92}Mo_{0.93}O_{5.69}$ [9], i.e. it consists of a ferrimagnetic arrangement of the Fe and Mo spins. The calculations of the magnetic moments

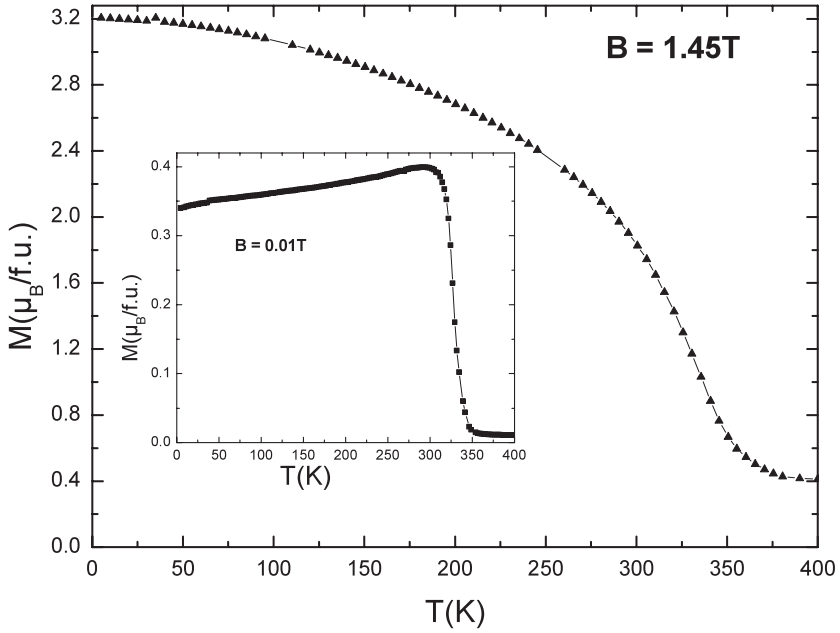

Figure 2. T-dependent magnetization (M) of the double perovskite Ba_2FeMoO_6, recorded in a field of 1.45 T (ZFC). The $M(T)$ curve in 0.01 T (ZFC) is also given in inset.

Table 1. Crystallographic parameters of Ba_2FeMoO_6, obtained by NPD refinements (λ = 1.2251 Å). Ba (0.25, 0.25, 0.25); Fe (0, 0, 0); Mo (0.5, 0.5, 0.5) and O (x, 0, 0).

	450 K $Fm3m$ 8.0851(1) Å	10 K $Fm3m$ 8.0506(2) Å
Ba B (Å^2)	0.59(2)	0.018(1)
Fe B (Å^2)	0.80(4)	0.158(1)
Mo B (Å^2)	0.37(5)	0.135(1)
O x	0.2581(2)	0.2563(1)
O B (Å^2)	0.88(2)	0.334(1)
M_{Fe} (μ_B)		3.7(1)
M_{Mo} (μ_B)		−0.5(1)
R_{Bragg}	3.24	3.03
R_f	2.87	1.49
R_{mag}		3.04
Selected interatomic distances (Å)		
Fe–O	2.087(1)	2.059(2)
Mo–O	1.956(1)	1.962(2)

of Fe and Mo were done artificially along y, i.e. without any physical meaning since the symmetry is cubic. They lead to 3.7 μ_B for Fe and −0.5 μ_B for Mo, in perfect agreement with the magnetization measurements (figure 2) which gave a value of 3.2 μ_B (10 K) per formula unit. These results were checked against data registered at 10 K on the G41 diffractometer (λ = 2.4266 Å) which has medium resolution but with a high flow. For these calculations, the crystallographic parameters were fixed to the values obtained from the 3T2 refinements, but the

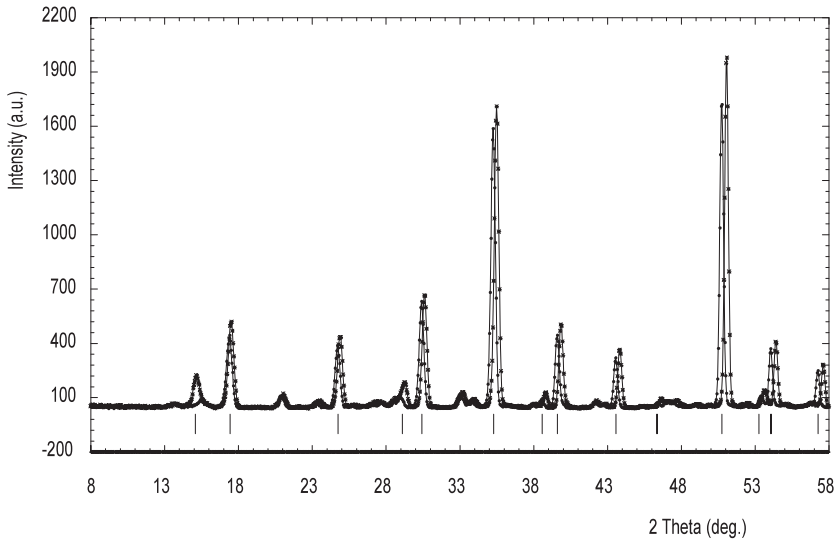

Figure 3. Neutron diffraction pattern ($\lambda = 1.225$ Å) registered at 10 K (crosses) and 450 K (circles) showing the mergence of nuclear and magnetic peaks. The Bragg sticks are only given for the main phase Ba_2FeMoO_6 ($Fm3m$).

Fe and Mo moments, as well as the lattice parameters and the scale factors for the three phases, were refined. The moments thus calculated are exactly the same as those previously obtained, i.e. 3.7(1) and $-0.5(1)$ μ_B for Fe and Mo respectively. This additional neutron diffraction registration is of prime importance for validating the high-resolution magnetic results.

The value of the magnetic moment of 3.2 μ_B is significantly smaller than that expected from the valencies of the cations, which should be close to 4 μ_B considering the pairs Fe^{2+} (higher spin, 4 μ_B)/Mo^{6+}(0 μ_B) or Fe^{3+} (higher spin, 5 μ_B)/Mo^{5+}(-1 μ_B). The latter result will be discussed later after description of the the x-ray absorption spectroscopy and Mössbauer studies, together with the Fe–O and Mo–O distances obtained from the NPD data.

X-ray absorption

In order to determine the Mo oxidation state we performed x-ray absorption spectroscopy of this compound at room temperature. This allows us to measure a given x-ray absorption near-edge spectrum of the cation inside complex materials and to compare the spectrum in the new material with that of the same cation in well known materials in which the environment is similar and the charge state well defined. Then direct measurement of the energies of the main absorption jump on the spectra of the reference compounds and of the compound under investigation will allow us to estimate the formal charge state in the material under investigation.

This technique was applied to the determination of the Mo charge state in Ba_2FeMoO_6 by measuring the Mo K-edge in the double perovskite and in $SrMoO_3$ perovskite, used as the reference oxide for Mo^{4+}, and $NaMo_3P_2O_{13}$ and $BaMo_2P_2O_{12}$ phosphates used as references for Mo^{5+} and Mo^{6+} respectively as described in [17] (figure 4). The energies of the half height of the main absorption jump are reported in table 2. As expected, the reference oxides clearly exhibit energy shifts towards high energy with the increase in Mo formal charge; the absorption edge of the studied double perovskite properly fits that of $BaMo_2P_2O_{12}$, showing that the formal charge of Mo in Ba_2FeMoO_6 must be close to 6+ within the experimental error

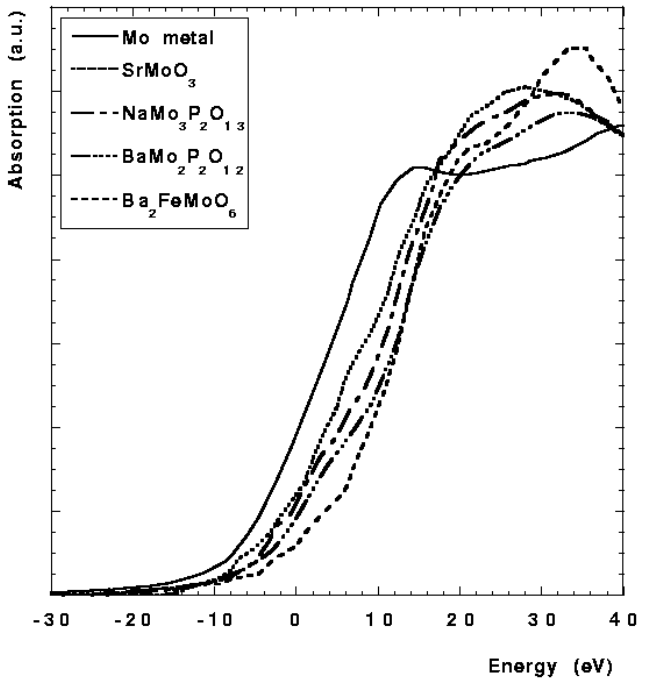

Figure 4. Mo K-absorption edges for three oxides containing Mo^{4+}, Mo^{5+} and Mo^{6+} charge states, and for the double perovskite Ba_2FeMoO_6, showing that Mo exhibits mainly the 6+ oxidation state.

Table 2. Energies of the midheight of the main absorption jump at the Mo K-edge for some reference compounds and for the double perovskite Ba_2FeMoO_6.

Compounds	Mo Formal charge in references	Midheight of main absorption jump (eV)	Expected Mo formal charge
Mo metal	0	2.4 ± 0.3	
$SrMoO_3$	4	8.3 ± 0.3	
$NaMo_3P_2O_{13}$	5	10.4 ± 0.3	
$BaMo_2P_2O_{12}$	6	12.5 ± 0.3	
Ba_2FeMoO_6		12.5 ± 0.3	6 ± 0.15

of ± 0.15. Consequently, a slight reduction of Mo formal charge with respect to 6+ cannot be completely ruled out.

The absence of any prepeak between 0 and 4 eV in the near-edge spectrum of Ba_2FeMoO_6 indicates that the local symmetry around Mo is quite different from that observed in molybdenum phosphates. This prepeak arises from an electronic transition from the Mo(1s) core level to the hybridized Mo(4d)–O(2p)–Mo(5p) molecular orbitals. The prepeak intensity is directly linked to the degree of hybridization of the Mo(4d) and O(2p) orbitals which increases with the distortion of the MoO_6 octahedron. The spectra of Mo^{5+} and Mo^{6+} phosphates exhibit a pronounced shoulder between 0 and 4 eV in agreement with the strong distortion of the Mo polyhedra, whereas the total absence of a shoulder in the spectrum of the double perovskite corresponds to a regular environment around Mo as observed from neutron diffraction analysis.

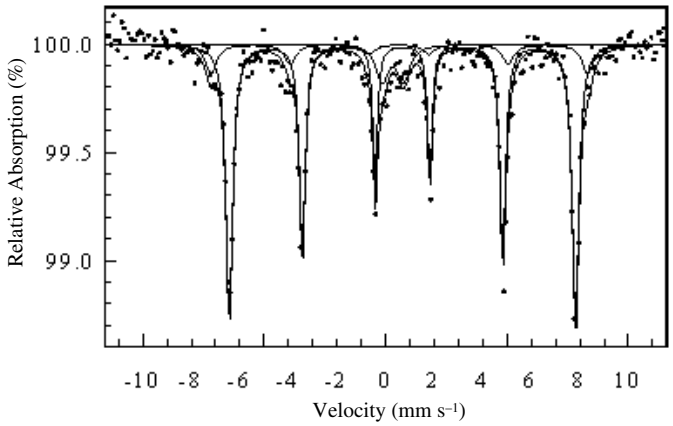

Figure 5. ^{57}Fe Mössbauer spectrum at 80 K of the Ba_2FeMoO_6 oxide.

Mössbauer spectrometry

The ^{57}Fe Mössbauer spectrum of Ba_2FeMoO_6, registered at 80 K (figure 5), is magnetically well resolved, in agreement with the T_C value above room temperature. One can distinguish a prevailing sextet with well resolved lines whose external lines exhibit anomalous broadening located at the outer wing, and in addition a quadrupolar component occurs in the low-velocity range. The main magnetic component has to be decomposed into two sextets with rather narrow Lorentzian lines, to describe the asymmetry of the outer lines. Such a description is consistent with that used for most low-temperature Mössbauer spectra obtained on those double perovskites. In addition, it is important to emphasize that the asymmetry of the outer lines cannot be accurately described by the fluctuating hyperfine field model used by Kim *et al* [13]. The corresponding hyperfine Mössbauer data (table 3) display two main magnetic components labelled A and B which have been classically fitted as sextet lines with a ratio of relative intensities of 3:2:1. The weak contribution labelled C (intensity $\approx 9\%$) may be due to the presence of a small number of superparamagnetic Fe^{3+} particles. This C site could correspond either to a superparamagnetic component ($\approx 9\%$) of Ba_2FeMoO_6 or to some non crystallized α-Fe_2O_3 residue with very small particles which cannot be detected by x-ray diffraction. In the study of Kündig and Bömmel [18], for 18 nm superparamagnetic α-Fe_2O_3 particles the quadrupole splitting (SQ) value decreases slightly from 0.44 to 0.39 mm s^{-1} in the range 296–80 K. Assuming the same decrease for smaller sized particles and owing to SQ = 0.98 mm s^{-1} given by these authors at 296 K for particles of less than 10 nm, one can estimate an SQ value close to 0.9 mm s^{-1} at 80 K for these latter particles, coherent with SQ (80 K) = 0.88 mm s^{-1} of our C component. Moreover, as the ratio Fe/Mo has been estimated as being 1 in our Ba_2FeMoO_6 by EDS and neutron diffraction, and owing to the excess of Mo (8%) in the $BaMoO_4$ impurity, it seems reasonable to attribute the C site to the 9% excess of Fe^{3+} as superparamagnetic α-Fe_2O_3.

As shown in table 3, the hyperfine parameters of the A and B sites at 80 K are consistent with those previously reported by Grenèche *et al* [7]. Our values for IS and the hyperfine field (B_{hyp}) at 80 K are smaller than those observed by those authors at 4.2 K, in agreement with the temperature effect. Unfortunately, data are difficult to compare since the previous authors did not check the composition of their 'Ba_2FeMoO_6' phase, using NPD, and used a different method of synthesis, similar to that described by Ritter *et al* [9].

In our 80 K Mössbauer spectrum, sufficiently important differences between both IS values ($IS_A = 0.82$ mm s^{-1}; $IS_B = 0.68$ mm s^{-1}) and B_{hyp} values ($B_{hyp(A)} = 44.3$ T,

Table 3. Fitted hyperfine Mössbauer data of our Ba_2FeMoO_6 and Sr_2FeMoO_6 samples and of [7]. IS: IS relative to metallic iron at room temperature. 2ε: quadrupole shift.

T (K)	Site	IS $\pm$ 0.02 mm s^{-1}	$2\varepsilon \pm 0.02$ mm s^{-1}	$B_{hyp} \pm 0.5$ T	% ± 5
Ba_2FeMoO_6					
80	A	0.82	0.01	44.3	77
	B	0.68	0.01	48.2	14
	C	0.41	0.88[a]	—	9
4 [7]		0.87	0.00	46.0	91
		0.72	0.10	49.7	9
Sr_2FeMoO_6					
4	A	0.70	−0.02	47.3	85
	B	0.67	−0.07	49.9	15
80	A	0.65	−0.01	45.8	86
	B	0.62	−0.04	47.7	14
473	A	0.50	0[a]	—	83
	B	0.31	0.34[a]	—	17
4.2 [7]		0.72	−0.02	47.7	68
		0.63	0.04	49.7	32
77 [7]		0.70	−0.01	46.2	70
		0.60	0.05	48.6	30
475 [7]		0.48	0.09[a]		63
		0.38	0.48[a]		37

[a] Quadrupole splitting in the paramagnetic domain.

$B_{hyp(B)} = 48.2$ T) lead us to conclude that the A and B valency states are not the same. First, x-ray absorption spectroscopy has shown that the Mo charge is close to 6+, which leads to a majority of Fe^{2+}/Mo^{6+} pairs in the compound; so, considering this result and the relative intensity of the A site, we can reasonably attribute an iron charge of 2+ for this main site ($\approx$80%). As regards the B site with lower IS and greater B_{hyp} values, a higher valence state close to 3+ can be expected. Note that coexistence of two different iron valence states in a same octahedral environment also occurs in the magnetite Fe_3O_4 which exhibits a spinel structure [19, 20]. These authors found that both Fe^{2+} and Fe^{3+} located in the octahedral sites of the spinel were split into two components. In a single crystal oriented parallel to the [111] axis, Berry *et al* found IS = 1.03 mm s^{-1} [20] at 4.2 K, for one of the two split Fe^{2+} components, which is higher than our A value. But in the work of Hargrove and Kündig [19] at 82 K, compatible with our experimental temperature (80 K), and under an external transverse field, the Mössbauer parameters (IS = 0.71 mm s^{-1}; $B_{hyp} = 47.3$ T) for this spinel octahedral split Fe^{2+} site lie in the same ranges as for our A and B components. These results lead us to think that the oxidation state of the A site is not exactly equal to 2+. Indeed, the presence of a small number of Fe^{3+}/Mo^{5+} pairs is consistent with the x-ray absorption results, owing to the lower limit of the experimental error (0.15) on the Mo charge.

The tendency of Ba_2FeMoO_6 to form an 'Fe^{2+}/Mo^{6+}' pair is strongly supported by the NPD data. At 450 K ($T > T_C$) in the paramagnetic state, the Fe–O distances of 2.087(1) Å are much higher than those observed at 500 K for Sr_2FeMoO_6 (1.996(4) Å) [9]. Simultaneously, the corresponding Mo–O bond at 450 K (1.956(1) Å) is smaller than for Sr_2FeMoO_6 at 500 K (1.966(4) Å) [9]. This evolution of interatomic distances is consistent with that reported for the $Ba_{2-x}Sr_xFeMoO_6$ series [9], confirming this general tendency, even if the analysed compositions are different in both studies due to a different synthesis process. This difference between the relative sizes of the FeO_6 and MoO_6 octahedra shows that in both compounds (Ba and Sr based) the Fe and Mo cations exhibit different charge states. Note that at 10 K the Fe–O distances in Ba_2FeMoO_6 (2.059(2) Å) are also significantly higher

than those previously observed [9] for Sr_2FeMoO_6 (1.979–2.027 Å), in agreement with the relative proportions of Fe^{3+} in those two oxides: about 20% Fe^{3+} for 'Ba' and a majority of Fe^{3+} for 'Sr' at low temperature. One observes that the size of the FeO_6 octahedra decreases as the temperature decreases whereas the size of the MoO_6 octahedra increases, indicating electronic transfer from Fe towards Mo as T decreases. Nevertheless, it must be emphasized that the temperature decrease induces more complex phenomena than a simple electronic transfer. The values of the magnetic moments obtained from the NPD data at 10 K, +3.7 μ_B for Fe and -0.5 μ_B for Mo, are indeed significantly different from those calculated on the basis of the Mössbauer results: 0.8 Fe^{2+} + 0.2 Fe^{3+} and 0.8 Mo^{6+} + 0.2 Mo^{5+}, which imply values of +4.2 and -0.2 μ_B respectively. The lower value for the moment obtained by NPD refinements for the Fe site is not in doubt, in contrast to the higher value refined on the Mo site. Let us note that small deviations which are too subtle to be determined with accuracy by our characterizations may be at the origin of such inconsistencies. For example a mis-site cationic disorder of 0.04 Fe^{3+} on the Mo site doubles the magnetic moment on this Mo site (0.04 Fe^{3+} + 0.76 Mo^{6+} + 0.2 Mo^{5+} $\rightarrow$ 0.4 μ_B). In the same way, by keeping the same Fe^{3+}/Fe^{2+} ratio, a small oxygen deficiency leads to an increase in the Mo^{5+}/Mo^{6+} ratio: the $O_{5.98}$ value obtained from the calculations gives a theoretical moment on the Mo site of 0.24 μ_B instead 0.2 μ_B for O_6. Clearly, other phenomena have to be taken into account when explaining the valence fluctuations at low temperature, according to the too simple equilibrium $Fe^{2+} + Mo^{6+} \Leftrightarrow Fe^{3+} + Mo^{5+}$: hybridization between O(2p) and Fe(3d) and O(2p) and Mo(4d) [21], but also, and very importantly, the existence of an antiferromagnetically coupled itinerant electron which would explain the metallic conductivity of this phase at low temperature [6].

In order to establish a better comparison with Sr_2FeMoO_6, we have revisited the Mössbauer properties of this phase prepared using our synthesis method in order to avoid large deviations from oxygen stoichiometry. The 4.2 and 80 K Mössbauer spectra (figure 6, table 3) show the existence of two magnetic components, labelled A and B, as in Ba_2FeMoO_6, but the presence of superparamagnetism can be neglected in the fits. From our results, and from those obtained by Grenèche *et al* [7], one observes that for both A and B sites there is a difference between the IS values, which are smaller in the Sr compound than in the Ba one. This difference appears more important for the major A site. Furthermore, the hyperfine fields B_{hyp} of this component (% A $\approx$ 86%) have higher values in the Sr sample. Let us note that it is not the structural transition (from cubic to tetragonal) observed in the Sr case that affects the carrier distribution. In fact in both cases the structures are described with FeO_6 and MoO_6 octahedra, which are regular in $Fm3m$ but slightly elongated along c in $P4_2/m$ [9]. These comparisons allow us to consider that the mean iron charge in the Sr oxide is greater than in the Ba one, in agreement with the electronic configuration $3d^{5.2}$ (i.e. $Fe^{2.8+}$) given by Grenèche *et al* [7], and close to that of Fe^{3+}. This result is furthermore confirmed by the spectrum recorded with a better statistic at high temperature 473 K (figure 7), above the magnetic transition (T_c = 422 K). One observes two paramagnetic doublets fitted by Lorentzian lines. Their IS values are close to those expected for trivalent iron (0.50 and 0.31 mm s^{-1}) and the relative intensities of these two sites are of the same order as those obtained at low temperature.

4. Concluding remarks

This study shows that the stoichiometric Ba_2FeMoO_6 double perovskite is characterized by a majority localized state of Fe^{2+} ions [$t_{2g}(3\uparrow) + t_{2g}(1\downarrow) + e_g(2\uparrow)$], corresponding to the couple Fe^{2+}–O–Mo^{6+}. This is in contrast to the Sr_2FeMoO_6 compound where the majority localized state involves Fe^{3+} ions ($t_{2g}{}^3\uparrow e_g{}^2\uparrow$), even in the paramagnetic state ($T > T_C$),

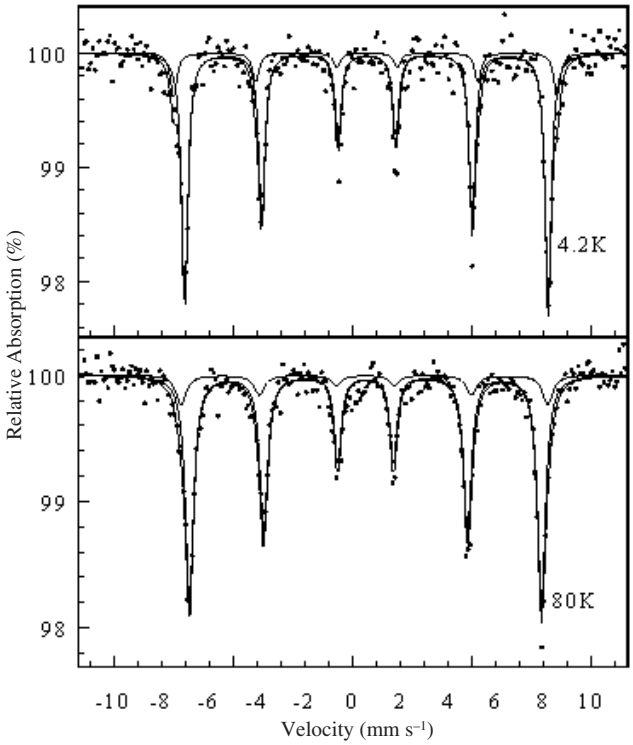

Figure 6. ^{57}Fe Mössbauer spectra at 4.2 and 80 K of Sr_2FeMoO_6.

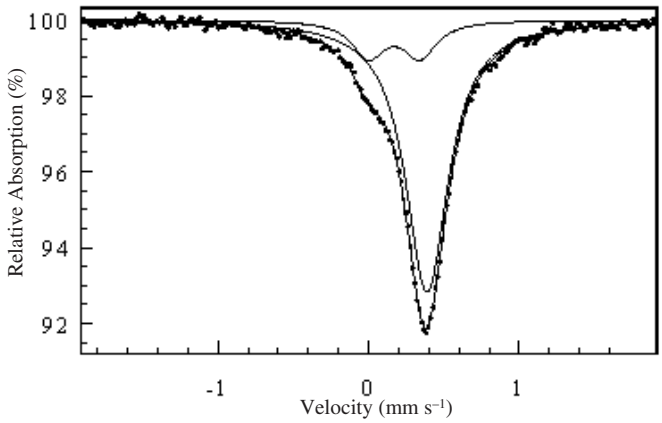

Figure 7. ^{57}Fe Mössbauer spectrum at 473 K of Sr_2FeMoO_6.

i.e. the couple Fe^{3+}–O–Mo^{5+}. Thus the size of the A site cation, Ba^{2+} or Sr^{2+} (1.61 and 1.44 Å respectively) [22], has a dramatic effect upon the nature of the low-temperature state, favouring the 'Fe^{2+}/Mo^{6+}' couple for large A cations and the 'Fe^{3+}/Mo^{5+}' for smaller ones. But in both cases an electronic transfer occurs as T decreases, whatever the nature of the high-temperature state (above T_C), Fe^{2+}/Mo^{6+} or Fe^{3+}/Mo^{5+}. Such a situation can be explained on the basis of the model developed by Kang *et al* [21], suggesting a tendency

to degeneracy of the localized Fe^{2+}/Mo^{6+} and Fe^{3+}/Mo^{5+} states, forming a minority $t_{2g}\downarrow$ narrow band '$Fe^{(2+\delta)+}$–O–$Mo^{(6-\delta)+}$' or '$Fe^{(3-\delta')+}$–O–$Mo^{(5+\delta')+}$', where the electron is itinerant, allowing a sort of double exchange mechanism, so that metallic conductivity appears at low temperatures. It is most probable that the 'Fe^{2+}/Mo^{6+}' state less easily degenerates into the '$Fe^{(2+\delta)+}/Mo^{(6-\delta)}$' band than the '$Fe^{3+}/Mo^{5+}$' state into '$Fe^{(3-\delta')}/Mo^{(5+\delta')}$', explaining the highest T_C of Sr_2FeMoO_6 compared with Ba_2FeMoO_6.

Acknowledgments

We are grateful to Professor M Hervieu for her efficient contribution to the EDS analyses and the electron diffraction experiments, and to Dr G André for the G41 data.

References

[1] Patterson F K, Moeller C W and Ward R 1963 *Inorg. Chem.* **2** 196
[2] Galasso F S, Douglas F C and Kasper R J 1966 *J. Chem. Phys.* **44** 1672
[3] Kobayashi K-I, Kimura T, Sawada H, Terakura K and Tokura Y 1998 *Nature* **395** 677
[4] Maignan A, Raveau B, Martin C and Hervieu M 1999 *J. Solid State Chem.* **144** 224
[5] Nakagawa T 1968 *J. Phys. Soc. Japan* **24** 806
[6] Lindén J, Yamamoto T, Karppinen M, Yamauchi H and Pietari T 2000 *Appl. Phys. Lett.* **76** 2925
[7] Grenèche J M, Venkatesan M, Suryanarayanan R and Coey J M D 2001 *Phys. Rev.* B **63** 174403
[8] Garcia-Landa B, Ritter C, Ibarra M R, Blasco J, Algarabel P A, Mahendiran R and Garcia J 1999 *Solid State Commun.* **110** 435
[9] Ritter C, Ibarra M R, Morellon L, Blasco J, Garcia J and De Teresa J M 2000 *J. Phys.: Condens. Matter* **12** 8295
[10] Goodenough J B and Dass R I 2000 *Int. J. Inorg. Mater.* **2** 3
[11] Tomioka Y, Okuda T, Okimoto Y, Kumai R, Kobayashi K-I and Tokura Y 2000 *Phys. Rev.* B **61** 422
[12] Ogale A S, Ogale S B, Ramesh R and Venkatesan T 1999 *Appl. Phys. Lett.* **75** 537
[13] Kim S B, Lee B W and Kim C S 2002 *J. Magn. Magn. Mater.* **242–245** 747
[14] Varret F and Teillet J, Université du Maine, unpublished
[15] Nassif V, Carbonio R E and Alonso J A 1999 *J. Solid State Chem.* **146** 266
[16] De Villiers J P R 1971 *Am. Mineral.* A **56** 758
[17] Savary L, Costentin G, Maugé F, Lavalley J C, Fallah J El, Studer F, Guesdon A and Ponceblanc H 1997 *J. Catal.* **169** 287
[18] Kündig W and Bömmel H 1966 *Phys. Rev.* **142** 327
[19] Hargrove R S and Kündig W 1970 *Solid State Commun.* **8** 303
[20] Berry F J, Skinner S and Thomas M F 1998 *J. Phys.: Condens. Matter* **10** 215
[21] Kang J-S, Han H, Lee B W, Olson C G, Han S W, Kim K H, Jeong J I, Park J H and Min B I 2001 *Phys. Rev.* B **64** 024429
[22] Shannon R D 1976 *Acta Crystallogr.* A **32** 751